ELSEVIER

Micron 35 (2004) 311–318

micron

www.elsevier.com/locate/micron

Purification of the recombinant hepatitis B virus core antigen (rHBcAg) produced in the yeast *Saccharomyces cerevisiae* and comparative observation of its particles by transmission electron microscopy (TEM) and atomic force microscopy (AFM)

Heng Chen[a,b,d,*], Jun Hong Lü[c], Wan Qi Liang[d], Ya Hong Huang[d,e], Wei Jie Zhang[a], Da Bing Zhang[d,*]

[a]*College of Life Science and Biotechnology, Shanghai Jiaotong University, Shanghai 200030,China*
[b]*School of Life Science, Shanghai University, Shanghai 200436,China*
[c]*Shanghai Institute of Applied Physics, Shanghai 201800, China*
[d]*Agro-Biotech Research Center, Shanghai Academy of Agricultural Sciences, Shanghai 201106,China*
[e]*Department of Biological Science and Technology, Nanjing University, Nanjing 210093, China*

Received 24 October 2003; revised 23 December 2003; accepted 23 December 2003

Abstract

Hepatitis B virus core antigen (HBcAg) gene (C gene) was expressed in *Saccharomyces cerevisiae* and the products (rHBcAg or core particles) were purified from a crude lysate of the yeast by three steps: Sephrose CL-4B chromatography, Sucrose step-gradient ultracentrifugation and CsCl-isopycnic ultracentrifugation. It has been observed that HBcAg was synthesized in yeast cells as a particle consisting of polypeptides with a molecular weight of 21.5 kDa (p21.5). Results of ELISA test and density analysis of CsCl-isopycnic ultracentrifugation indicated that the purified products (rHBcAg particles) with HBcAg antigenicity mainly located at the densities of 1.27 and 1.40 g ml^{-1}, respectively. Observation and analysis of the purified rHBcAg products by TEM indicated that rHBcAg peptides could mainly self-assemble into two size classes of core particles. The larger particles were ~30.1 nm and the smaller were ~21.5 nm in mean diameter. Further observation and analysis of the same rHBcAg (core) particles by AFM also indicated that rHBcAg (core) particles were similar to the native HBcAg (core) particles from infected human hepatocytes and mainly composed of two size classes of partides core. The larger particles were ~31.3 nm and the smaller were ~22.5 nm in mean diameter which was similar to the results obtained by TEM. All results from both TEM and AFM suggested that core particles (capsids) produced in *S. cerevisiae* possessed dimorphism.

Keywords: rHBcAg purification; *Saccharomyces cerevisiae*; rHBcAg (core) particles (capsids); Transmission electron microscopy; Atomic force microscopy; Dimorphism

1. Introduction

Hepatitis B virus (HBV) is a member of the Hepadnavirus family and is the etiologic agent of acute and chronic liver disease in human. HBV is a small DNA virus with a lipid–protein envelope surrounding an icosahedral nucleocapsid. The nucleocapsid consisting of HBcAg protein (core protein) plays a vital role in the life cycle of the virus and in the morphogenesis of the double-shelled HBV virion. HBcAg protein is a major viral nucleocapsid protein consisting of a 19–21.5 kDa polypeptide, which shares the antigenic sites responsible for both HBc and HBe

Abbreviations: rHBcAg, recombinant hepatitis B core antigen; EM, electron microscopy; TEM, transmission electron microscopy; AFM, atomic force microscopy; ELISA, enzyme-linked immunosorbent assay; HBV, hepatitis B virus; HBcAg, HBV core antigen; HBeAg, HBV e antigen; *anti*-HBc, antibody to HBcAg; 2D, two-dimensional; 3D, three-dimensional; SD, synthetic dropout; *S. cerevisiae, saccharomyces cerevisiae*; STEM, scanning transmission electron microscopy.

* Corresponding authors. Tel.: +86-216-2934292; fax: +86-21-32170043.

E-mail addresses: dr.chenheng@163.com (H. Chen); zdb30@hotmail.com (D.B. Zhang).

0968-4328/$ - see front matter © 2004 Elsevier Ltd. All rights reserved.
doi:10.1016/j.micron.2003.12.003

antigens (Takayuki et al., 1988). The exact length of HBcAg protein depends on the HBV genotype. As the carboxy-terminal region of this peptide is rich in basic amino acids, it has been assumed that the HBcAg peptide can bind non-specifically RNA and encapsidate specifically pregenomic HBV RNA. The C-gene has two initiation codons separated by 87 bp in the same reading frame, and the polypeptides produced by translation from the upstream and downstream initiation codons consist of 212 and 183 amino acids, respectively (Fujiyama et al., 1983). HBcAg protein has the ability to form disulfide-linked homodimers, which spontaneously assemble into particles (Zhou and Standring, 1992). Native hepatitis B virus core particles from human liver visualized by negative staining have been reported to have diameters of 27–30 nm and an icosahedral appearance (Onodera et al., 1982). HBcAg is a very powerful immunogen inducing strong humoral, T helper (Th) and cytotoxic T-cell (CTL) responses and functioning as both T-cell-dependent and T-cell-independent antigen (Milich et al., 1997a,b). Intensive studies have shown that HBcAg can be produced in a variety of heterologous expression systems including *Escherichia coli* and Yeast, and then undergoes correct folding and self-assembly to form core particles similar to native capsids (Pasek et al., 1979; Cohen and Richmond, 1982; Naito et al., 1997; Wizemann and Von Brunn, 1999). HBcAg molecules expressed in bacteria assemble into particles of two size arranged, respectively, with a triangulation number $T = 3$ (90 dimers) or $T = 4$ (120 dimers) icosahedral symmetry (Crowther et al., 1994; Wingfield et al., 1995). The physiological implications of this dimorphic switch are not clear, although the $T = 4$ form is reported to outnumber the $T = 3$ form by ~13-1 in capsids isolated from the human liver (Kenney et al., 1995). The crystal structure of the $T = 4$ capsids of the bacterially expressed truncated protein (aa 1–149) has been solved by X-ray crystallography to 3.3 Å resolution (Wynne et al., 1999). The monomer fold is characterized by four α-helices and the absence of β-sheets. In agreement with previous biochemical analyses, the structure data revealed two regions required for the dimerization of core monomers and for the subsequent assembly of the dimers into core particles (Wynne et al., 1999). Although we still understand very little about the molecular interactions that underlie the various steps of HBV virion assembly, it is almost certain that specific core protein residues are intimately involved in drawing the viral polymerase and RNA pregenome into the assembling nucleocapsid, while a different set of residues presumably direct the envelopment of the finished core particle by a coat of viral surface protein and lipid (Seifer and Standring, 1995). Nucleocapsid assembly takes place in the cytoplasm and is initiated around a complex of viral mRNA and HBV reverse transcriptase (Nassal and Schaller, 1993). Since nucleocapsid assembly itself involves mutiple sets of contacts, first between core protein monomers to form dimers and then between dimers to form higher structures, it is apparent that a study of the viral core protein necessarily entails the delineation of a wealth of protein–protein and protein–nucleic acid interactions. Moreover, it gives us an opportunity to study the masking and presentation of epitopes that accompanies assembly and disruption of nucleocapsids. In previous researches on core particles (capsids), except those micrographs of HBcAg particles obtained by transmission electron microscopy (TEM), cryo-TEM and X-ray crystallography (Crowther et al., 1994; Wingfield et al., 1995; Wynne et al., 1999), there are no native pictures of HBcAg particles directly imaged in air or liquor reported. The problem of HBcAg imaged in air or liquid has been solved since invention of atomic force microscopy (AFM). It is unlikely that any probe technology such as scanning transmission electron microscopy (STEM) or AFM can compete with cryogenic electron microscopy (EM) or X-ray crystallography as a means of delineating virus structure, particularly the interior structure. Nonetheless, AFM may have its place in accurately determining the dimensions of virus particles, their mechanical properties and the architecture of their surface. In the best of cases, it may be capable of revealing capsomere arrangements and perhaps even the distribution of capsid protein subunits within the capsomeres (Kuznetsov et al., 2001). Because AFM can be applied under physiological conditions, it captures the particles in a natural state without the distortions imposed by drying, fixing or staining. In general speaking, heights of single particles on mica and centre-to-centre distance of particles in ordered arrays are the most reliable measures of a virion's dimensions. If these are used, shapes and dimensions obtained by AFM agree well, to within a few percent, with results based on cryogenic EM and X-ray structure determination. Moreover, different viruses can be discriminated from one another based on shape, size and capsomere structure. Resolution of very closely related viruses would probably not be possible at this time. Nonetheless, AFM can give some useful information regarding the presence or distribution of different viruses in a sample (Kuznetsov et al., 2001). As AFM technology progresses and better, it has been a promising tool for biological application and occupies a unique position among the methods of direct visualization available to the biologist today. It combines the high spatial resolution of electron microscopes with the ability of optical microscopes to image biological samples under vacuum, gaseous or aqueous environments, thus avoiding the harsh and damaging preparative and imaging procedure used in conventional methods of electronic microscopy and X-ray crystallography. However, AFM also has limits in biological application, it cannot always to image all biomolecules at a molecular resolution (Ziegler et al., 1998; Wilkinson et al., 1999). To directly observe the native images of HBcAg particles in air and investigate the probable dimorphism of rHBcAg (core) particles produced in yeast *Saccharomyces cerevisiae*, in this paper, we reported the TEM and AFM images and dimorphic analysis of rHBcAg (core) particles derived from yeast *S. cerevisiae*.

2. Materials and methods

2.1. Recombinant plasmid and expression strain

The recombinant plasmid PEJ24 in which HBcAg gene was integrated. PEJ24 was constructed and provided by Liang wanqi of Agro-Biotech Research Center, Shanghai Academy of Agricultural Sciences. The expression strain EGY48 was the yeast *S. cerevisiae* with PEJ24.

2.2. Key enzymes, reagent and kit

The key reagents and SD culture medium for growth of yeast *S. cerevisiae* were bought from Shanghai Perfect Biotechnology Ltd; HBeAg test kits for ELISA were produced by Shanghai Kehua Biotechnology Ltd; In western blotting, the first antibody was polyclonal rabbit anti-HBcAg (1:100 dilution) bought from Neomarkers Co. of America; the secondary antibody was alkaline phosphatase-conjugated goat anti-rabbit IgG (1:5000 dilution) bought from Promega Co. of America; the nitrocellulose filter was made by Amersham Co. of England.

2.3. Key experiment instruments

The Sepharose CL-4B column was made by Pharmacia Co. of Sweden; the ultracentrifuge was a Sorvall Ultra Pro80 Superspeed centrifuge made by Sorvall Co. of America; the enzyme-linked assay instrument was a Bio-rad model 550 microplate reader made by Bio-rad Co. of America; the TEM was a CM120 (BioTWin, CRYO) TEM made by Philips, Eindhoven, The Netherlands; the AFM was a Multimode nanoscopy IIIa AFM made by Digital Instruments, USA.

2.4. Expression of HBcAg gene in yeast *Saccharomyces cerevisiae*

The yeast *S. cerevisiae* strains EGY48 stored in −70 °C refrigerator were revived and streak plated on SD-trp plates, cultured at 30 °C for 2–5 days. The recombinant yeast monocolony from SD-trp plates was grown in shaker flask with 5 ml SD medium at 30 °C overnight, and the culture was transferred into the shaker flask with 200 ml SD medium, cultured at 30 °C overnight until the $A_{600\ nm}$ reached 4–6. The 200 ml of culture was transferred into the small fermentor with 20 l SD medium and cultured at a stirring speed of 1000 rpm at 30 °C for 3–4 days.

2.5. Collection of expression strains and separation of rHBcAg (core) protein

The culture fluid was collected and in batches centrifuged in rotor RPR10-2-335 by the centrifuge (HITACHI 20PR-5 Japan) at 3000 rpm for 5 min, every pellet with the yeast cells was pooled and finally about 80 g yeast pellet was obtained from 20 l of culture. The yeast pellet was washed three times with cold distilled water, resuspended at 0.2 g/ml (wet yeast biomass) in cold lysis buffer (10 mM $MgCl_2$, 0.3 M $(NH_4)_2SO_4$, 20 mM Tris–HCl pH7.9, 1 mM EDTA pH8.5, 1 mM DTT, 5% Glycerol) with 500 μm quartz sand and disrupted by ultrasound in one 2 s pulse for 10 min. After disruption, cell suspension was separated from the quartz sand and debris by centrifugation at 13,000 rpm at 4 °C for 30 min. The supernatant was collected and subjected to ammonium sulfate precipitation, 50% saturation, at 4 °C for 4–6 h. The precipitated fraction was isolated by centrifugation at 13,000 rpm at 4 °C for 30 min and then dissolved in 5 mM Tris–HCl (pH7.4) buffer and dialyzed against the same buffer overnight. Finally contaminants were removed by centrifugation at 13,000 rpm at 4 °C for 30 min and the supernatant containing the HBc protein was cryo-concentrated, tested by ELISA and stored at 4 °C.

2.6. ELISA assay

ELISA assay of sample was performed according to the protocol of HBeAg test kits, which were made in Shanghai Kehua Biotechnology Ltd of China. Added 60 μl of samples, positive and negative controls to appropriate wells of the coated microplates (96 well microtiter plate); then added 60 μl of monoclonal antibody enzyme conjugate to each well except negative control well and completely mixed the content of each well. Covered the plate and incubated at 37 °C for 30 min. Aspirated solution from each well. Washed the microplate 3–5 × with 200 μl per well of Wash Solution and tap on absorbent paper to remove all excess liquid after the final wash. Added 60 μl of streptavidin-HRP and TMB, respectively, to each well and incubated in the dark at 37 °C for 15 min. Stopped the reaction by addition of 60 μl of Stop Solution to each well. Finally read microplate at 450 nm within 10 min of adding Stop Solution and the result of ELISA reaction was judged as a positive result according to this computing formula: $OD_{450\ nm}$s of sample/ $OD_{450\ nm}$s of negative control ≥ 2.1.

2.7. Preliminary purification of rHBcAg (core) protein

For preliminary purification, a Sepharose CL-4B column (600 × 20 mm; Pharmacia, Sweden) was used. TE (10 mM Tris–HCl pH 7.4, 1 mM EDTA) buffer was used as an eluent at the following linear flow-rate: 0.3 ml/min. A 3-ml Sample was clarified by centrifugation prior to injection on the column. Each eluant fraction was subjected to ELISA for detection of core antigen. The ELISA positive fractions were pooled, subjected to ammonium sulfate precipitation, 50% saturation, at 4 °C for 4–6 h. The precipitated fraction was isolated by centrifugation at 12,000 rpm at 4 °C for 30 min and then dissolved in 5 mM Tris–HCl (pH 7.4) buffer and dialyzed against the same buffer overnight. Finally contaminants were removed by centrifugation at

12,000 rpm at 4 °C for 30 min and the supernatant containing the rHBc protein was cryo-concentrated, and stored at 4 °C.

2.8. Western blotting analysis

After electrophoresis, the proteins in a polyacrylamide gel were electrophoretically transferred onto a nitrocellulose filter according to the method of Towbin (Towbin et al., 1979). Immediately following transfer, the western blotting was undertaken according to the method of Sambrook (Sambrook et al., 1989) described in the book 'Molecular Cloning'.

2.9. Sucrose step-gradient ultracentrifugation

In order to purify the rHBc core particles, the prepurified extract of *S. cerevisiae* EGY48 was subjected to sucrose discontinuous gradient centrifugation. TH-614 12-ml polyallomer tubes (Sorvall Co., USA) were filled successively with 1.5 ml of decreasing sucrose solution (60, 50, 40, 30, 20, 10%, w/w). Each sucrose gradient fraction was, respectively, formed in 10 mM Tris–HCl (pH 7.4) buffer (including 1 mM EDTA pH 8.0 and 0.2% TritonX-100). Then 1 ml of prepurified extracts was layered on the top of each tube. Centrifugation was performed at 32,000 rpm in a Sorvall type TH-614 rotor (Sorvall Co., USA) at 4 °C for 22 h. The gradients were drained by pipetting 0.5-ml fractions and subjected to protein analysis and ELISA testing. The fractions with higher ELISA reaction intensity were pooled and dialyzed against 5 mM Tris–HCl (pH 7.4) buffer overnight, cryo-concentrated for standby.

2.10. CsCl-isopycnic ultracentrifugation

For further purification of the rHBc core particles, rHBc solutions (500 μl) were layered on top of a CsCl gradient consisting of 5 ml of 40% (w/v) CsCl in 5 mM Tris–HCl (pH 7.4) buffer and 5 ml of 10% (w/v) CsCl in the same buffer in a 12-ml polyallomer tube, and centrifuged at 30,000 rpm in a Sorvall type TH-614 rotor (Sorvall Co. USA) at 4 °C for 60 h. The gradients were drained by pipetting 0.5 ml fractions and subjected to protein analysis and ELISA testing. The density of individual fraction was determined by the refractive index using a WZS1 Abbe refractometer. The fractions with higher ELISA reaction intensity were pooled and dialyzed against 5 mM Tris–HCl (pH 7.4) buffer overnight, lyophilized and stored at 4 °C.

2.11. Transmission electron microscopy of rHBcAg (core) particles

The purified and lyophilized rHBcAg sample was dissolved with 10 μl 5 mM Tris–HCl (pH 7.4) buffer. Put a drop of the suspension of sample to be stained on a sheet of Parafilm. Floated a formvar-carbon coated 300 mesh copper grid on the drop (filmed side down) for 5 min. Removed the grid, and drained off excess liquid by touching edge to a piece of clean filter paper. Touched the grid (filmed side down) to a drop of phosphotungstic acid (PTA, pH 6.5) for about 3–5 min, and drained off excess as before. Allowed to dry a few minutes, then examined using a Phillips CM120 TEM with an acceleration voltage of 90 kV.

2.12. Atomic force microscopy of rHBcAg (core) particles

The purified and lyophilized rHBcAg sample was dissolved with 100 μl 5 mM Tris–HCl (pH 7.4) buffer, the concentration of this solution was 6.316 mg/ml by measurement of ultraviolet spectroscopy at 280 and 260 nm, and diluted 1:1000 with the same buffer. A 10 μl drop of a diluted rHBcAg particle solution was deposited onto freshly cleaved mica. After a waiting time of 10–15 min, the surface of mica was rinsed by three times with redistilled water to remove salts and unattached molecules, and then dried for approx. 15 min with clean dry airflow until the surface appeared dry. The dried mica with sample was kept in the neat dryer overnight. In the second day, the mica surface with sample was used for AFM studies. The AFM instrument was a Nanoscope IIIa Multimode scanning probe microscope (Digital Instruments Co., Santa Barbara, CA, USA). Images were obtained at ambient temperature and humidity. The tapping mode and standard silicon cantilevers 90 μm length were employed for imaging in air. The cantilever oscillation frequency was turned to the resonance frequency of approx. 330 kHz. We generally adjusted the set point voltage for optimum image quality. Both height and phase information were recorded at a scan rate of 2 Hz, and stored in either 256 × 256 pixel format. Images were processed using the Nanoscopy version 5.12 software.

3. Results

3.1. Expression and characterization of rHBcAg produced in yeast Saccharomyces cerevisiae

To characterize rHBcAg derived from yeast *S. cerevisiae*, samples of the primarily purified rHBcAg were subjected to SDS-PAGE and Western blotting analysis using polyclonal antibody-rabbit anti-HBcAg (1:100 dilution) and alkaline phosphatase-conjugated goat anti-rabbit IgG (1:5000 dilution). As shown in Fig. 1, the result indicates that HBcAg gene successfully was expressed in the yeast *S. cerevisiae* and produced a protein whose molecular weight was approx. 21.5 kDa, as judged from its mobility in comparison with those of standard proteins. This value agrees with that deduced from the DNA sequence. This p21.5 also shares the antigenic epitope responsible for HBc antigens.

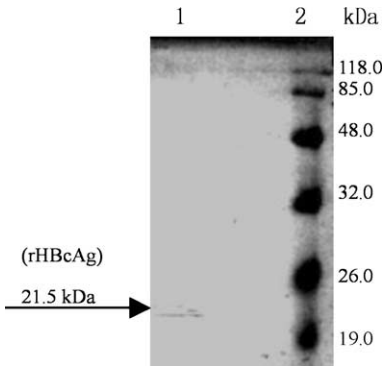

Fig. 1. Western blot analysis of HBc gene expression. (1) Expression products of EGY48/pBJ24-L; (2) protein marker.

3.2. Sucrose step-gradient ultracentrifugation

To purify the rHBcAg (core) particles, the sucrose step-gradient ultracentrifugation was performed according to the previous method. As shown in Fig. 2, the result indicates that the fraction 3, 4, 5, 6, 7 and 8 were higher in ELISA reaction intensities, and six of these fractions were pooled for further purification.

3.3. CsCl-isopycnic ultracentrifugation

The CsCl-isopycnic ultracentrifugation was performed according to the previous method. As shown in Fig. 3, the result indicates that the fractions with higher ELISA reaction intensities were the fraction 3 and 11, and with density of 1.27 and 1.40 g ml^{-1}, respectively. The fraction 3 and 11 were pooled for TEM detection of the viral core particles.

3.4. Transmission electron microscopy of rHBcAg (core) particles

By electron microscopy (EM), it is shown that two main size classes of core particles were assembled from rHBcAg. Both the larger and the smaller particles exhibited spherical native-like core particles from the HBV-infected human liver. The mean diameter of the larger particles was 30.1 nm with standard deviation of 2.4 nm and the smaller was 21.5 nm with standard deviation of 3.3 nm ($n = 148$ particles; see Fig. 4). Among the 148 core particles, there were 72 larger and 76 smaller particles, respectively. It seems to suggest that the proportion of two main size classes of core particles simultaneously produced in yeast *S. cerevisiae* approaches to one.

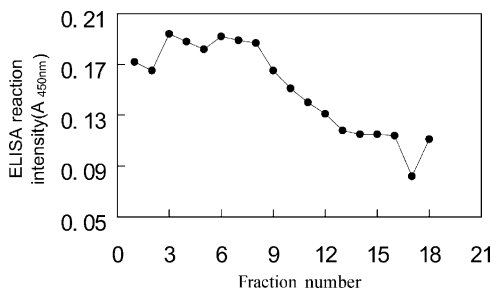

Fig. 2. ELISA reaction intensity ($A_{600\ nm}$) of rHBcAg (core) particles in each fraction.

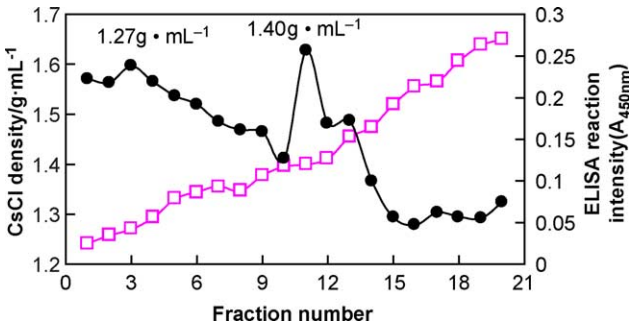

Fig. 3. ELISA reaction intensity (●) and CsCl density (□) of rHBcAg (core) particles in each fraction.

3.5. Atomic force microscopy of the rHBcAg (core) particles

For detection of core particles by AFM, it was necessary to dilute the core particle solution 1:1000 to obtain satisfactory AFM images. In this study, we used a stock solution of core particles at approx. 6.316 μg ml^{-1}. We developed a novel direct detection method for the images of core particles by AFM imaging. Figs. 5a and 6a show tapping mode AFM images of air-dried core particles of difference size on the mica surface. Fig. 6b shows simulated three-dimensional (3D) images corresponding to Fig. 6a. Fig. 5b shows the distribution of core particles with different size from off-line particle analysis of AFM images of core particles. Statistical analysis indicates that most of the core particle sizes centre on 22.5 and 31.3 nm, respectively (Fig. 5b). It is also indicated that the core particles mainly consist of two size species of particles and quantities of the smaller core particles exceed those of the larger. From these results, it seems to suggest that recombinant HBcAg or core particles (capsids) produced in *S. cerevisiae* also display the dimorphism like in *E. coli*. (Crowther et al., 1994). Fig. 6a shows two size species of core particles, the smaller particle is ~28.3 nm and the larger is ~32.2 nm in diameter by off-line section analysis of the particles. Fig. 6b shows the simulated 3D AFM images of two core particles. It is obviously indicated that the typical core particles with different height are two size species of core particles.

4. Discussion

It has been shown that rHBcAg (core) particles can be purified in term of our methods. Western blotting and ELISA tests have confirmed that the *S. cerevisiae*-derived HBcAg (core) particles possess the characteristic antigenic properties of both HBcAg and HBeAg. Results of these

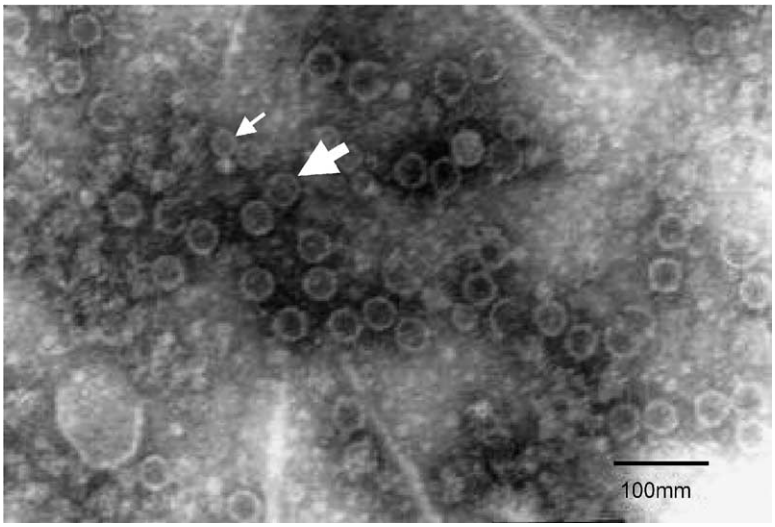

Fig. 4. Transmission electron microscopy showing negatively stained purified rHBcAg (core) particles derived from *S. cerevisiae*. (× 133200). The bar in the micrograph represents 100 nm large white arrow indicates the large core particle; Small white arrow indicates the small core particle.

studies and of other confirmatory tests will be reported elsewhere. Preliminary density gradient studies have shown that the *S. cerevisiae*-derived HBcAg (core) particles mainly give bands at 1.27 and 1.40 g ml^{-1}, respectively, in caesium chloride, indicating that probably there are two size classes of core particles derived from *S. cerevisiae*, but at present, it is not sure that these core particles of main two sizes exactly locate in the bands with densities of 1.27 and 1.40 g ml^{-1}, respectively, and further study is required. For further observation of the core particles, besides TEM technique, we have used the recently developed technique of AFM to examine the core particles produced by transformed yeast cells, and have further compared AFM micrographs of these particles with TEM micrographs obtained by negative staining. To our knowledge, the sizes of viral capsids can be flattened and shrinked by negative staining in TEM (Crowther et al., 1994; Yamaguchi et al., 1988b), while in AFM, for roughly spherical particles, such as icosahedral viruses, although their diameter appears greater than is in fact the case, the vertical height of the particles gives a remarkably accurate value for their true diameter (Kuznetsov et al., 2001). In our study, we substituted particle analysis for section analysis in off-line measures of core particle diameters. On the one hand, in particle analysis, measures of core particle diameters are based on the vertical height of the particles, on the other hand, in section analysis, measures of core particle diameters are based on the lateral width of the particles. It is evident that the diameter of core particle appears greater in section analysis than in particle analysis. Even though there is a flattening effect of air-drying on the core particles in preparation of sample for AFM in air, the particle diameters based on vertical measurements approach to their actual diameters. In previous work, native HBcAg particles (capsids) from

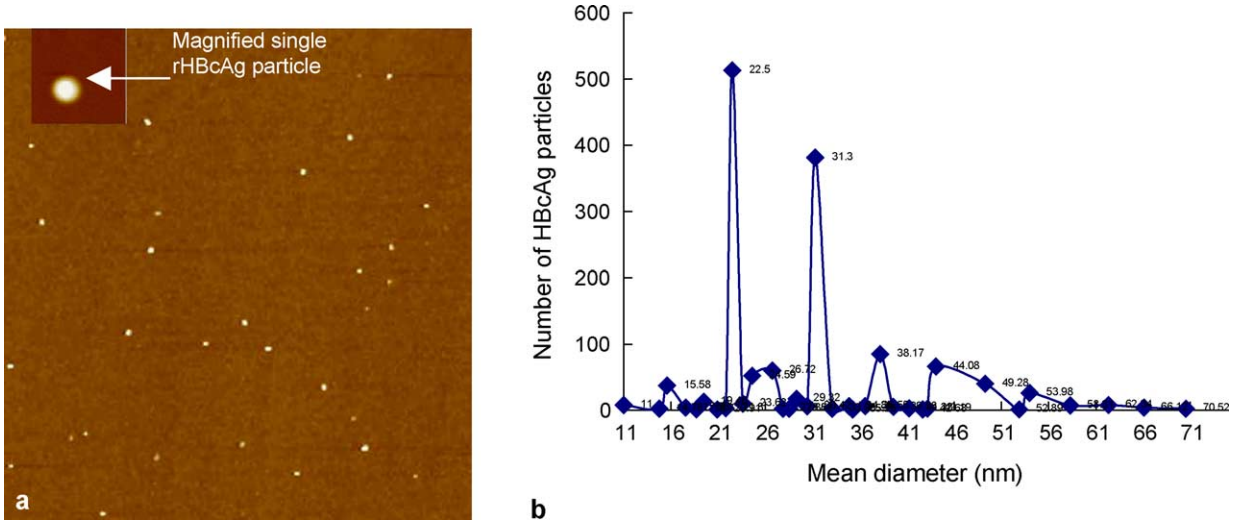

Fig. 5. AFM image and size distribution of rHBcAg (core) particles. (a) AFM 2D image of many dispersed core particles. (Scan size 5 μm × 5 μm) and a magnified single rHBcAg particle. (Scan size 150 nm × 150 nm). (b) The size distribution of core particles.

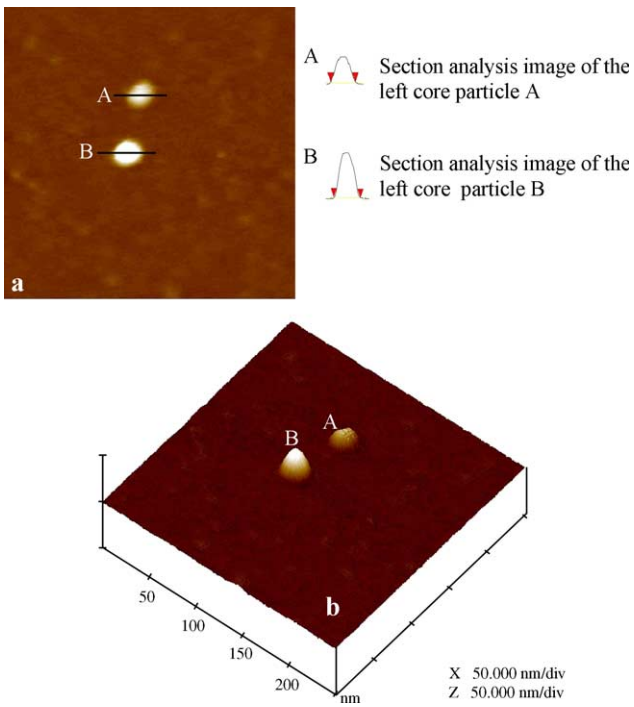

Fig. 6. AFM images of two rHBcAg (core) particles with different size. Scan size 250 nm × 250 nm. (a) AFM 2D image and section analysis of two core particles with different size. A: the smaller core particle is about 28.3 nm in diameter; B: the larger core particle is about 32.2 nm in diameter. (b) Simulated 3D image of core particle A and B in Fig. 6a.

human liver visualized by negative staining have been reported to have diameters of about 27–30 nm and an icosahedral appearance (Onodera et al., 1982). Similar dimensions and morphologies have also been reported for recombinant HBcAg (core) particles produced in *E. coli* (Edman et al., 1981; Cohen and Richmond, 1982; Bènèdicte et al., 2002); in yeast (Miyanohara et al., 1986; Takayuki et al., 1988; Yamaguchi et al., 1988a); in insect cells with a baculovirus expression vector (Hildrich et al., 1990); and in a *xenopus* oocyte system (Zhou and Standring, 1991). *E. coli*-derived core particles visualized by negative staining were reported to have average diameters of about 27.3 nm by Cohen and Richmond (1982) or 34 nm by Bènèdicte et al. (2002), while *S. cerevisiae*-derived core particles visualized by negative staining were reported to have average diameters of about 27 nm by Takayuki et al. (1988) or 31.3 nm by Yamaguchi et al. (1988a,b). In this paper, we found that *S. cerevisiae*-derived larger core particles visualized by negative staining TEM and non-staining AFM had average diameters of about 30.1 and 31.3 nm, respectively, which was similar to the results obtained by Yamaguchi et al. (1988a,b).

Previous work has established that the bacterially expressed core protein assembles to give two different sizes of shell, composed of 180 or 240 subunits arranged with $T = 3$ or 4 icosahedral symmetry, respectively, and with subunits paired to produce dimeric spikes protruding from the surface of the shell. Usually, the quantities of the larger shell exceed that of the smaller (Crowther et al., 1994). Wingfield et al. (1995) had also reported the same $T = 3/T = 4$ dimorphism of core particles derived from *E. coli* by using STEM and analytical ultracentrifugation. It is not yet known whether native HBcAg particles (capsids) located in the HBV core or as uncoated capsids in the infected hepatocytes and blood, exhibit the same $T = 3$ (small)/$T = 4$ (large) dimorphism. As yet, we do not know the physiological implications of this dimorphic switch. Additionally, the difference in diameter between these two variants of core particles is slight and cannot be determined with confidence by conventional electron microscopic methods. This case will be well resolved with application of AFM. In our study, we developed a novel direct detection method for the rHBcAg (core) particles in air by AFM imaging. Core particles deposited onto mica could be reliably imaged by AFM and AFM images could clearly reveal the 2D and simulated 3D images of rHBcAg (core) particles (capsids). It was especially important that the core particles produced in *S. cerevisiae* had been confidently determined by using AFM to have the same dimorphism as in *E. coli*. Furthermore, the result of detection and statistical analysis of core particles by AFM nearly accorded with that by TEM. However, the proportion of the two size classes of core particles varied slightly from the statistical method of AFM to that of TEM. This difference could result from the discrepancy of statistical ways of AFM and TEM. In general, the statistical method of particle quantities in AFM is more objective and believable than in TEM. In addition, the question remains as to why the proportion of the two size classes of core particles produced in *S. cerevisiae* reverse that of those produced in *E. coli*. The further research on this case is required.

Acknowledgements

The authors would like to gratefully thank Professor Jun Hu for his supervision and help in nanotechnology. We also thank Juan Yang for her technical assistance in culture of yeast.

References

Bènèdicte, W., Martine, Q., Dominique, R., Gaspard, G., Marie, G., Michel, J., Odile, L., 2002. Characterization and diagnostic potential of hepatitis B virus nucleocapsid expressed in *E. coli* and *P. pastoris*. J. Virol. Method 102, 175–190.

Cohen, B.J., Richmond, J.E., 1982. Electron microscopy of hepatitis B core antigen synthesized in *E. coli*. Nature 296, 677–678.

Crowther, R.A., Kiselev, N.A., Böttcher, B., Berriman, J.A., Borisova, G.P., Ose, V., Pumpens, P., 1994. Three-dimensional structure of hepatitis B virus core particles determined by electron cryomicroscopy. Cell 77, 943–950.

Edman, J.C., Hallewell, R.A., Valenzuela, P., Goodman, H.M., Rutter, W.J., 1981. Synthesis of hepatitis B surface and core antigen in *E. coli*. Nature 291, 503–506.

Fujiyama, A., Miyanohara, A., Nozaki, C., Yoneyama, T., Ohtomo, N., Matsubara, K., 1983. Cloning and structural analyses of hepatitis B virus DNAs, subtype adr. Nucleic Acids Res. 11, 4601–4610.

Hildrich, C.M., Rogers, L.J., Bishop, D.H.L., 1990. Physiocochemical analysis of the hepatitis B virus core antigen produced by a baculovirus expression vector. J. Gen. Virol. 71, 2755–2759.

Kenney, J.M., von Bonsdorff, C.H., Nassal, M., Fuller, S.D., 1995. Evolutionary conservation in the hepatitis B virus core structure: comparison of human and duck cores. Structure 3, 1009–1019.

Kuznetsov, Y.G., Malkin, A.J., Lucas, R.W., Plomp, M., Mcpherson, A., 2001. Imaging of viruses by atomic force microscopy. J. Gen. Virol. 82, 2025–2034.

Milich, D.R., Chen, M., Schodel, F., Peterson, D.L., Jones, J.E., Hughes, J.L., 1997a. Role of B cells in antigen presentation of the hepatitis B core. Proc. Natl Acad. Sci. USA 94, 14648–14653.

Milich, D.R., Schodel, F., Hughes, J.L., Jones, J.E., Peterson, D.L., 1997b. The hepatitis B virus core and e antigens elicit different Th cell subsets: antigen structure can affect Th cell phenotype. J. Virol. 71, 2192–2201.

Miyanohara, A., Imamura, T., Araki, M., Sugawara, K., Ohtomo, N., Matsubara, K., 1986. Expression of hepatitis B virus core antigen gene in *Saccharomyces cerevisae*: synthesis of two polypeptides translated from different initiation codons. J. Virol. 59, 176–180.

Naito, M., Ishii, K., Nakamura, Y., Kobayashi, M., Takada, S., Koike, K., 1997. Simple method for efficient production of hepatitis B virus core antigen in *E. coli*. Res. Virol. 148, 299–305.

Nassal, M., Schaller, H., 1993. Hepatitis B virus replication. Trends Microbiol. 1, 221–228.

Onodera, S., Ohori, H., Ishida, N., 1982. Electron microscopy of human hepatitis B virus cores by negative staining-carbon film technique. J. Med. Virol. 10, 147–155.

Pasek, M., Goto, T., Gilbert, W., Zink, B., Schaller, H., MacKay, P., Leadbetter, G., Murray, K., 1979. Hepatitis B virus genes and their expression in *E. coli*. Nature 282, 575–579.

Sambrook, J., Fritsch, E.F., Maniatis, T., 1989. Molecular Cloning: A Laboratory Manual, second ed., Cold Spring Harbor Laboratory Press, New York.

Seifer, M., Standring, D.N., 1995. Assembly and antigenicity of Hepatitis B virus core particles. Intervirology 38, 47–62.

Takayuki, I., Keishin, S., Satoshi, A., Yoshinobu, M., Hiroshi, M., Tadao, M., 1988. Purification and characterization of the hepatitis B virus core antigen produced in the yeast *Saccharomyces cerevisae*. J. Biotech. 8, 149–162.

Towbin, H., Staehelin, T., Gordon, J., 1979. Electrophoretic transfer of proteins from polyacrylamide gels to nitrocellulose sheet: procedure and some application. Proc. Natl Acad. Sci. USA 76, 4350–4354.

Wilkinson, K.J., Balnois, E., Leppard, G.G., Buffle, J., 1999. Characterization feature of the major components of freshwater colloidal organic matter revealed by transmission electron and atomic force microscopy. Colloid Surface 155, 287–310.

Wingfield, P.T., Stahl, S.J., Williams, R.W., Steven, A.C., 1995. Hepatitis core antigen produced in *E. coli*: subunit composition,conformational analysis, and in vitro capsid assembly. Biochemistry 34, 4919–4932.

Wizemann, H., Von Brunn, A., 1999. Purification of *E. coli*-expressed HIS-tagged hepatitis B core antigen by Ni^{2+} chelate affinity chromatography. J. Virol. Meth. 77, 189–197.

Wynne, S.A., Crowther, R.A., Leslie, A.G., 1999. The crystal structure of the human hepatitis B virus capsid. Mol. Cell 3, 771–780.

Yamaguchi, M., Hirano, T., Sugahara, K., Mizokami, H., Araki, M., Matsubara, K., 1988a. Electron microscopy of hepatitis B virus core antigen expressing yeast cells by freeze-substitution fixation. Eur. J. Cell. Biol. 47, 138–143.

Yamaguchi, M., Hirano, T., Hirokawa, H., Sugahara, K., Mizokami, H., Matsubara, K., 1988b. Cryo-electron microscopy of hepatitis B virus core particles produced by transformed yeast: comparison with negative staining and ultrathin sectioning. J. Electron Microsc. 37 (6), 337–341.

Zhou, S., Standring, D.N., 1991. Production of hepatitis B virus nucleocapsid-like core particles in *Xenopus oocytes*; assembly occurs mainly in the cytoplasm and does not require the nucleus. J. Virol. 65, 5457–5464.

Zhou, S., Standring, D.N., 1992. Cys residues of the hepatitis B virus capsid protein are not essential for the assembly of viral core particles but can influence their stability. J. Virol. 66, 5393–5398.

Ziegler, U., Vinckier, A., Kernen, P., Zeisel, D., Semenza, G., Murer, H., Groscurth, P., 1998. Preparation of basal cell membranes for atomic force microscopy. FEBS Lett. 436, 179–184.